**Astronomy
&
Astrophysics**

Adsorption of CO on amorphous water-ice surfaces

A. Al-Halabi[1,3,★], H. J. Fraser[2], G. J. Kroes[1], and E. F. van Dishoeck[3]

[1] Leiden Institute of Chemistry, Gorlaeus Laboratories, Leiden University, PO Box 9502, 2300 RA Leiden, The Netherlands
[2] Raymond and Beverly Sackler Laboratory for Astrophysics at Leiden Observatory, PO Box 9513, 2300 RA Leiden, The Netherlands
[3] Leiden Observatory, PO Box 9513, 2300 RA Leiden, The Netherlands
    e-mail: ewine@strw.leidenuniv.nl

Abstract. We present the results of classical trajectory calculations of the adsorption of thermal CO on the surface of compact amorphous water ice, with a view to understanding the processes governing the growth and destruction of icy mantles on dust grains in the interstellar medium and interpreting solid CO infrared spectra. The calculations are performed at normal incidence, for $E_i = 0.01$ eV (116 K) and surface temperature $T_s = 90$ K. The calculations predict high adsorption probabilities (∼1), with the adsorbed CO molecules having potential energies ranging from −0.15 to −0.04 eV with an average energy of −0.094 eV. In all the adsorbing trajectories, CO sits on top of the surface. No case of CO diffusion inside the ice or into a surface valley with restricted access was seen. Geometry minimizations suggest that the maximum potential energy of adsorbed CO (−0.155 eV) occurs when CO interacts with a "dangling OH" group, associated with the 2152 cm^{-1} band seen in laboratory solid-state CO spectra. We show that relatively few "dangling OH" groups are present on the amorphous ice surface, potentially explaining the absence of this feature in astronomical spectra. CO also interacts with "bonded OH" groups, which we associate with the 2139 cm^{-1} infrared feature of solid CO. Our results for CO adsorption on amorphous ice are compared with those previously obtained for CO adsorption to crystalline ice. The implications of the spectroscopic assignments are discussed in terms of the solid-CO infrared spectra observed in interstellar regions. Using the Frenkel model, the lifetime τ for which CO may remain adsorbed at the surface is calculated. At temperatures relevant to the interstellar medium, i.e. 10 K, it is longer than the age of the universe, but decreases dramatically with increasing T_s, such that at $T_s = 90$ K, $\tau = 300$ ns. The pre-exponential factor τ_ν used in the Frenkel model is found to be 0.95 ± 0.02 ps. These data are compared to recent experimental results. The astrophysical implications of these calculations are discussed, with particular reference to the CO binding sites identified on amorphous ice surfaces, their adsorption energies, probabilities and lifetimes.

Key words. astrochemistry – line: identification – molecular data – molecular processes – ISM: molecules – ISM: lines and bands

1. Introduction

Surface reactions occurring on or at ice surfaces have received significant attention in many different research fields, including astrochemistry. In dense regions of the interstellar medium, i.e. star-forming regions and dark clouds, heterogeneous reactions are believed to occur at the surface of icy dust grains. These grains typically consist of silicate or carbonaceous cores, covered by ice, predominantly H_2O, in addition to other molecules such as CO, CO_2, NH_3 and CH_4 (Ehrenfreund & Schutte 2000). Infrared observations have revealed that H_2O and CO are usually the most abundant molecules present in the mantles (Tielens et al. 1991; Tanaka et al. 1994; Chiar et al. 1995; Allamandola et al. 1999). Therefore, the simplest model of interstellar ice can be considered as the CO-H_2O binary-ice system, both for theoretical and experimental studies. An appreciation of the physical interplay between these two ice

constituents is a first step in understanding the behavior of interstellar ices, particularly in interpreting infrared observations, modelling ice growth and destruction in astrochemical models, and accounting for the wealth of molecular species that are formed through surface reactions.

Interstellar H_2O ice is believed to be predominantly amorphous in structure (Hagen et al. 1981). The specific morphology of amorphous interstellar H_2O ice remains an open question, particularly when referring to its porosity, given that H_2O is thought to form at the grain surface through chemical reactions rather than via gas phase condensation. It is usually assumed, however, that the structure closely resembles that of interstellar ice grown by vapor deposition in the laboratory, known as Amorphous Solid Water (ASW), rather than those ice phases formed under high pressure conditions, such as high density amorphous ice (hda) and low density amorphous ice (lda) (Petrenko & Whitworth 1999; Ehrenfreund et al. 2003). Experimentally, vapor-deposited H_2O ices are

---
★ Also known as A. Al-Remawi.

therefore universally employed as suitable analogs of the interstellar case, also because their growth can be controlled to obtain amorphous ices of varying porosity, at specific surface temperatures and angles of incidence (Kimmel et al. 2001). The work presented here focuses on amorphous H_2O ice, which is modelled to closely resemble compact, non-porous, vapor-deposited, amorphous solid water. This novel model is described in detail in Sect. 3.1.

The presence of solid CO is generally inferred by a broad absorption feature at around 2139 cm^{-1} (4.675 μm), and has been observed along many lines of sight towards the dense regions in the interstellar medium, the galactic center and high and low mass young stellar objects (Tanaka et al. 1994; Chiar et al. 1994, 1995; Whittet et al. 1998; Boogert et al. 2000; Boogert et al. 2002a,b; Pontoppidan et al. 2003). Assuming that interstellar ices are intimately mixed, these observations show that along every line of sight, CO seems to reside in two distinct ice environments: the first, revealed by a broad band at 2139 cm^{-1}, has historically been assigned to CO in van der Waals bonded ice (also referred to as H_2O-poor or "apolar" ice in the literature), such as pure CO ice; the second, revealed by a band at 2136 cm^{-1} was related to CO in hydrogen bonded ice (also known as H_2O-rich or "polar" ice), such as H_2O ice. Results from laboratory experiments on mixed H_2O and CO ice systems (summarized in detail in Sect. 2) suggest that when CO is incorporated within an H_2O ice, its infrared spectrum is dominated by a band at 2136 cm^{-1}, whereas pure CO ice spectra are dominated by a feature at 2139 cm^{-1}. The mixed H_2O-CO ices also often show a strong 2152 cm^{-1} feature in the laboratory.

Pontoppidan et al. (2003) have recently surveyed solid CO towards 39 low and intermediate mass young stellar objects at higher spectral resolution and S/N than previous studies. A phenomenological analysis of their data shows that all spectra can be decomposed into contributions of three differently weighted components, centered at 2143.7 cm^{-1}, 2139.9 cm^{-1} and 2136.5 cm^{-1}. The first two components at 2143.7 cm^{-1} and at 2139.9 cm^{-1} indicate that between 60 and 90% of the CO is present in its "pure" form. Since the CO is condensed from the gas phase, this suggests that most of the solid CO exists in multi-layers on top of the H_2O, with a small fraction present at the ice-CO interface, as opposed to being mixed in with other ice constituents. Furthermore, by following feasible evolutionary scenarios, Pontoppidan et al. (2003) show that some of the CO probably migrates from this pure over-layer into the porous H_2O ice below, becoming trapped there, as also suggested by recent experimental data (Collings et al. 2003b). The observations indicate that on average about 16% of the solid-CO can be trapped within the H_2O matrix in this way, resembling an ice mixture. Their third spectral component at 2136.5 cm^{-1} is in part attributed to this trapped CO. The 2152 cm^{-1} feature is never observed in astronomical spectra.

It is therefore of direct relevance to examine the interactions between gas-phase CO molecules and H_2O ice surfaces: first, to understand the growth of CO over-layers on H_2O ice surfaces; second, to gain chemical insight into the possible surface adsorbing sites and their corresponding binding energies and then to associate this to understanding of the interstellar

infrared features of solid CO; and third, to investigate the adsorption probability and lifetime of CO on the surface and thus its potential to participate in other heterogeneous surface reactions, for example to form solid CO_2 or CH_3OH.

In this paper, we present new theoretical results, using classical trajectory calculations, pertaining to the adsorption of CO on H_2O ices. Specifically, molecular dynamics simulations, commonly used in the physics and chemistry communities to study gas-surface interactions, are performed to determine the adsorption probability of CO on amorphous ice. Such calculations are capable of determining the energy transfer to-, and the energy dissipation within- the surface, due to atomic and molecular collisions or molecule formation at the surface. For molecules adsorbed at the surface within the time scale of the trajectory calculation (typically a few picoseconds, see Figs. 1b and 1c), the binding site can be identified, and the binding energy between the molecule and the surface calculated. From an analysis of the binding sites occupied in these calculations, it is possible to corroborate the experimental assignments of the spectroscopic bands observed when CO is adsorbed on H_2O, which may be compared directly with astronomical infrared observations. By running a statistically significant number of trajectories, the distribution of binding sites and energies is obtained: a comparison between "backscattering" (Fig. 1a) and "adsorbing" (Figs. 1b and 1c) trajectories gives the adsorption probability.

It is important to note that the adsorption probability computed by classical trajectory calculations is not necessarily directly comparable to the adsorption probability measured under experimental conditions or that relevant for astrophysical situations, since molecules that may be adsorbed at the end of a trajectory may later desorb, and therefore not contribute to the final surface coverage as measured experimentally (compare Figs. 1b and 1c). Using the Frenkel model (Frenkel 1924), which is also commonly used in astrochemistry (Augason 1970; Goodman 1978; Tielens & Allamandola 1987; Pirronello et al. 1997), the effects of surface temperature on the lifetime of the adsorbed CO molecule can be calculated from the classical trajectory results and extrapolated to interstellar conditions. Geometry minimizations of CO interacting with a static amorphous ice are also performed to find the detailed molecular structure of the adsorption sites, and their corresponding binding energies. Here, "static ice" means that the water molecules of the ice surface are at fixed positions. Our results for CO adsorbed to amorphous ice are compared with previous theoretical results obtained for CO interacting with crystalline ice (Al-Halabi et al. 2003b), and with the results of experimental studies on the system. All these data are directly relevant to the formation of interstellar ice mantles, and can be implemented in observational or astrochemical models where ice mantle growth and desorption are important.

From a theoretical perspective, several previous molecular dynamics simulations have been performed on amorphous and crystalline H_2O ice surfaces, generating results relevant to the interstellar medium, although none to date has focused on the H_2O-CO system under astrochemically relevant conditions. Calculations have been performed to model the growth of amorphous ice clusters of irregular shapes and various sizes
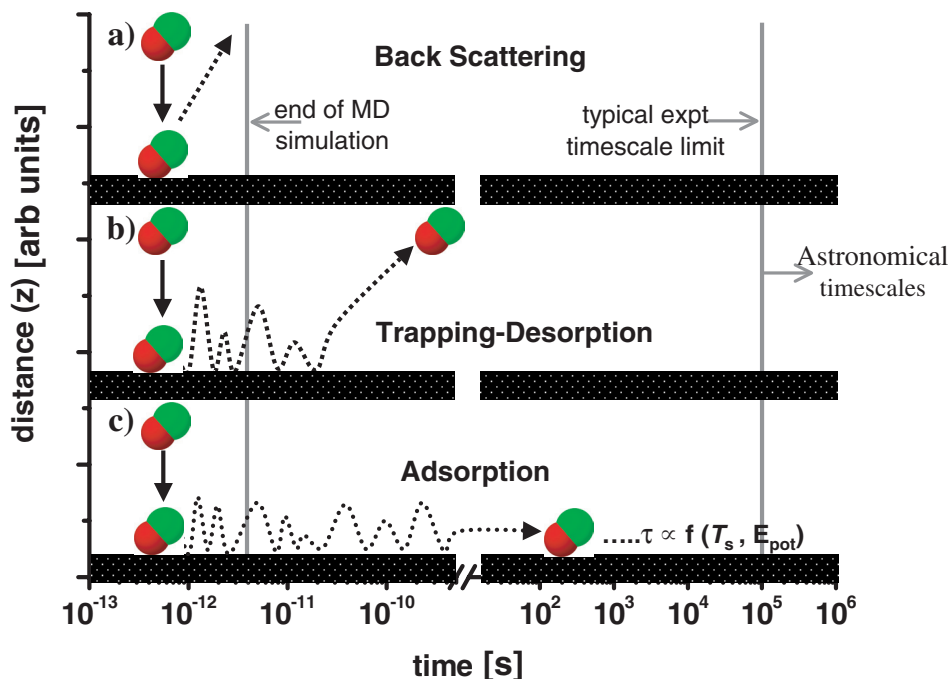
Fig. 1. Comparison between the timescales and definitions in classical trajectory calculations and experimental data (see text for details). MD stands for molecular dynamics.

(Zhang & Buch 1990; Buch 1990, 1992) and to simulate infinitely extending surfaces of high or low density amorphous ice, applying periodic boundary conditions (Takahashi et al. 1999a,b). The adsorption of H and D atoms on amorphous (Buch & Zhang 1991; Masuda et al. 1998) as well as crystalline (Al-Halabi et al. 2002) ice surfaces has been studied using molecular dynamics and classical trajectory techniques. The adsorption, formation, and desorption of H_2 has also been simulated on amorphous ice using classical techniques (Hixson et al. 1992; Takahashi et al. 1999a; Takahashi & Williams 2000).

The remainder of this paper is organized as follows: in Sect. 2, an overview of previous experimental and theoretical work on the CO-H_2O ice system is presented, the infrared spectroscopy of the system is discussed, and the possible adsorbing sites are identified. In Sect. 3, we present the methods used in this study. The results and the astrochemical implications are discussed in Sect. 4 and the key findings are summarized in Sect. 5.

2. Laboratory spectroscopy and theoretical studies of CO-H_2O ices

2.1. Water ice surfaces and definition of CO adsorbing sites

To investigate the nature of the possible CO adsorbing sites on ice surfaces, it is first necessary to understand the morphology of the H_2O ice surface. Based on its pair interactions with other H_2O molecules, each water molecule in the surface can be labelled by the number of the hydrogen bonds it forms with the neighboring water molecules. As an illustration, Figs. 2a and 2b show a portion of the uppermost

(surface) bilayer of a crystalline ice slab. The water molecules in the first monolayer are classified as three-hydrogen bonded molecules. These molecules can have six possible orientations, as shown in Fig. 2. In three orientations, the water molecule has one of its OH groups pointing upwards away from the surface. This OH group is labelled as "dangling OH" (Fig. 2). The second OH group, labelled as "bonded OH", is pointing obliquely down, forming a hydrogen bond with a water molecule in the second monolayer. In the other three orientations, the water molecule has both its OH groups pointing obliquely down to the water molecules in the second monolayer: both these OH groups are classified as "bonded OH" in this case. The lone pairs of electrons on the oxygen atoms of these water molecules provide the so-called dO adsorbing site for CO (Devlin & Buch 1995). In the second monolayer, each water molecule forms four-hydrogen bonds, so all the OH groups are involved in the hydrogen bonding network, and can also be labelled as "bonded OH". The molecules in this second surface monolayer provide the s4 adsorbing sites for CO (Devlin & Buch 1995), see Fig. 2.

Unlike crystalline water ice, amorphous water ice shows no long range order, so the adsorbing sites discussed above, involving CO adsorption on a "dangling OH" site or on a water oxygen atom (dO and s4 adsorbing sites), are more difficult to identify. We have therefore chosen to discuss the possible adsorbing sites of CO according to its interactions with the water hydrogen atoms, i.e. the OH groups. According to this viewpoint, CO can either interact with a "dangling OH", or with a "bonded OH". On crystalline ice, once CO is adsorbed at either a dO or a s4 site, it effectively interacts with "bonded OH" groups. Therefore, the dO and s4 adsorbing sites can also be identified as "bonded OH" sites, according to our alternative labelling. Given that the CO-H_2O interaction energy is
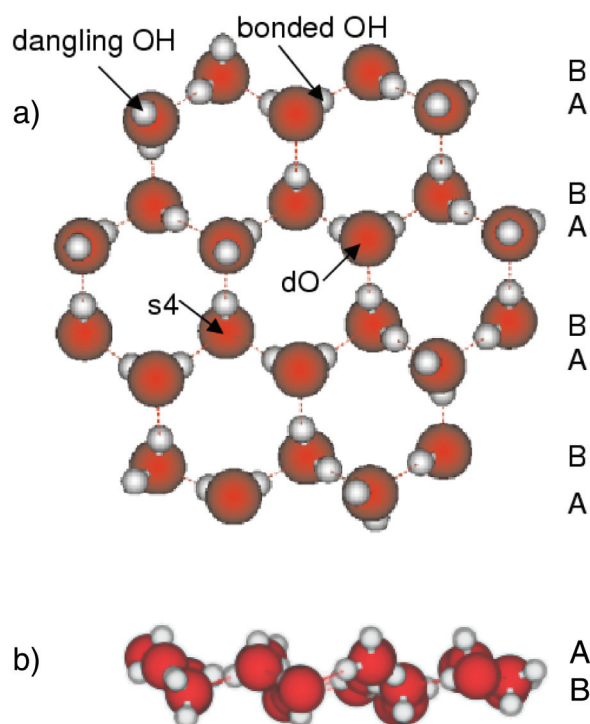
Fig. 2. a) Top and **b)** side views of a portion from the first bilayer of a crystalline ice surface showing the possible adsorbing sites for CO. The molecules are shown in (A) the top and (B) the bottom monolayer of the surface bilayer. Dotted lines show the hydrogen bonding network. See the text for more details.

attractive when CO interacts with the H-atom and repulsive when CO interacts with the O-atom of the water molecule (see below, Fig. 3 and Sect. 3.2), and given the lack of structure in the amorphous ice surface, this makes a direct comparison between the binding sites and adsorption behavior of CO on amorphous and crystalline ices simpler.

2.2. CO-H_2O infrared spectroscopy

When CO is incorporated inside a H_2O ice at 10 K, usually by co-deposition of a gas mixture, or simultaneous deposition of CO and H_2O, the infrared profile of the CO shows two features at about 2138 cm^{-1} and 2152 cm^{-1} (Sandford et al. 1988). The 2138 cm^{-1} band has been attributed to substitutional CO, i.e. CO replacing a water molecule within the matrix, and the 2152 cm^{-1} band to interstitial CO, i.e. CO between the water molecules (see Table 1). As such a mixed ice is warmed, the 2152 cm^{-1} band decreases in intensity, disappearing completely by around 80 K: the primary band shifts from 2138 to 2136 cm^{-1}, decreasing slightly in intensity. It is important to note that both these features are associated with CO *in* the ice matrix, not *on* the ice surface.

However, as noted in the introduction, interstellar spectra are more accurately reproduced by layered ices. In laboratory experiments, the infrared profile of multilayers of CO, adsorbed on top of an amorphous ice at T_s = 10 K, show a feature at 2139 cm^{-1} (dominated by CO-CO interactions in the multilayer but with a contribution from CO-H_2O interactions

at the ice-ice interface), and a significantly lower intensity feature at 2152 cm^{-1} (related to CO-H_2O interactions at the ice-ice interface) (see references below). The infrared profiles of sub-monolayer coverages of CO on amorphous ices at T_s = 10 K also show a feature at 2139 cm^{-1} and a lower intensity feature at 2152 cm^{-1}, both of which are related to CO-H_2O interactions at the ice-ice interface. It is important to note that the CO-H_2O and CO-CO 2139 cm^{-1} features can only be distinguished from each other by tracing their temperature evolution. At sub-monolayer coverages CO desorbs from the H_2O ice surface as the ice is warmed, such that above 50−80 K CO is no longer adsorbed for any appreciable time *on* the ice surface and the CO-H_2O 2139 cm^{-1} feature is not detected: on the other hand, as multilayers of CO on porous amorphous ices are warmed, trapping and desorption compete, so some of the CO becomes incorporated in the H_2O matrix as its porous structure collapses, and the CO-H_2O 2139 cm^{-1} feature decreases in intensity, shifts to around 2136 cm^{-1}, and narrows. This band is then indistinguishable from the 2136 cm^{-1} feature in mixed ices, and is related to CO *in* the water matrix (see Table 1).

The definite assignment of the interactions giving rise to these surface features came from a series of clever experiments in which pre-adsorbates, such as CF$_4$, CHF$_3$, or ethylene oxide, were used to block certain sites on crystalline ice surfaces. These molecules all bind more strongly to the ice than CO, so that the available adsorbing sites can be selected prior to CO adsorption (Devlin 1992; Graham et al. 1999). For example, if ethylene oxide is pre-adsorbed to the ice surface, it forms a hydrogen bond with a "dangling OH" group, thereby blocking the adsorbing sites that correspond to the 2152 cm^{-1} band (Devlin 1992). Consequently, in experiments where CO is adsorbed to the ethylene oxide-ice system, the 2152 cm^{-1} band is never observed (Devlin 1992). Conversely, molecular dynamics simulations for crystalline ice show that CF$_4$ resides at the center of the surface hexagonal rings (similar to CHF$_3$ Graham et al. 1999), blocking the water shafts and leaving only the dangling OH sites accessible (Buch et al. 1996). In that case, the 2152 cm^{-1} band is seen first experimentally at low CO exposures, and its infrared signal is more intense than that of the 2139 cm^{-1} band, in contrast to the case of CO adsorption on a clean ice surface (Devlin 1992; Martin et al. 2002b). This is a direct result of many of the dO and 4s adsorbing sites being blocked by the pre-adsorbed CF$_4$. At higher CO coverage, the signal of the primary band at 2139 cm^{-1} dominates due to CO-CO interactions, similar to the case of multilayer CO adsorption on clean ice (Martin et al. 2002b).

All of the previous experimental and theoretical studies thereby converged on the assignment of the 2152 cm^{-1} band to CO adsorbed at a dangling OH binding site, (Devlin 1992; Palumbo 1997; Manca et al. 2000; Manca & Allouche 2001; Martin et al. 2002a; Collings et al. 2003b), and a molecular configuration with CO perpendicular to the surface with its C-atom pointing downwards (Allouche et al. 1998). However, the molecular configuration of the 2139 cm^{-1} CO-H_2O "binding site" remains an open question. The first experiments specifically investigating CO adsorption to H_2O surfaces attributed this band to CO absorbed in the ice pores (Devlin 1992). Alternatively, adsorption isotherm Fourier transform
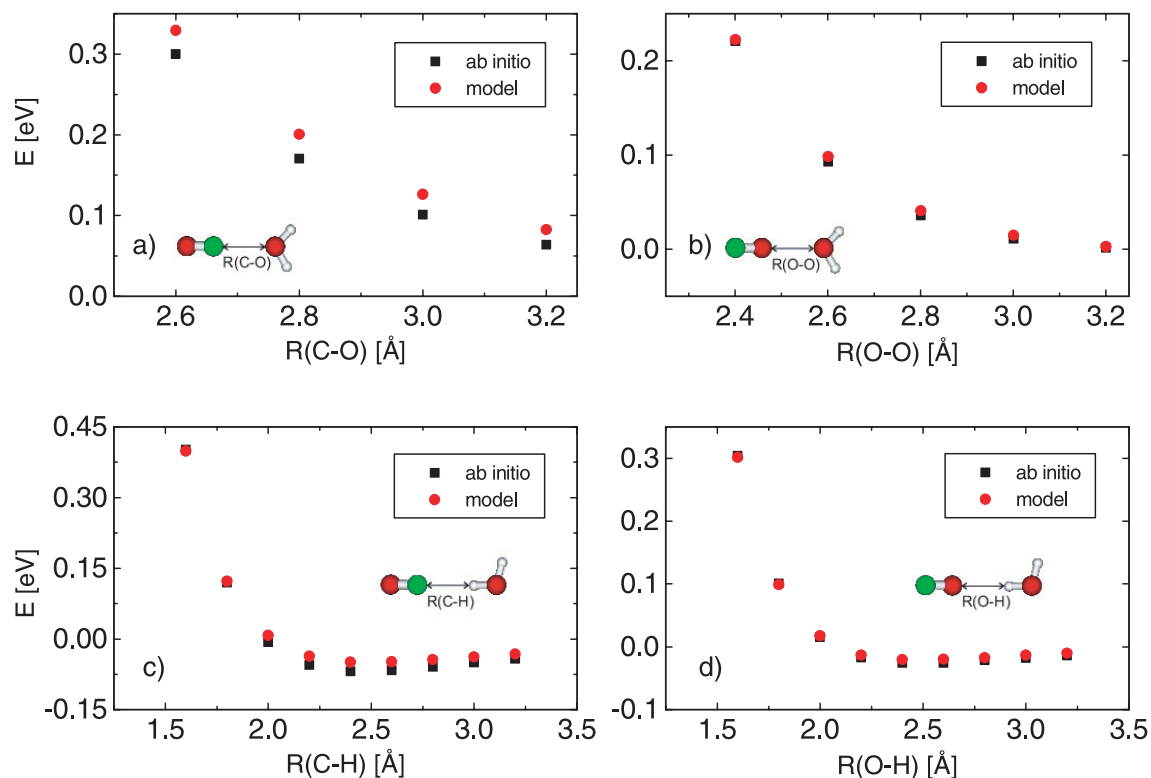
Fig. 3. Interaction energies of the CO-H$_2$O complex obtained from the pair potential fit, plotted together with energies of the complex obtained from ab initio calculations. Energies are plotted as a function of the distance between the closest atoms of the interacting molecules, i.e. **a)** OC-OH$_2$, **b)** CO-OH$_2$, **c)** OC-HOH, and **d)** CO-HOH. The dark spheres represent the O-atom, the grey spheres the C-atoms, and the small light-grey spheres the H-atoms.

Table 1. Summary of current assignments of CO-H$_2$O spectral features in the CO stretching region

Approx. frequency (cm^{-1})	Comment	Assignment	Molecular configuration	Astronomical spectra
MIXED ICE				
2152		CO in H$_2$O	Interstitial CO[a] CO-dangling OH?[#]	No
2138–2136	irreversibly shifts & narrows as T raised	CO in H$_2$O	Substitutional CO[a#]	Only at 2136 cm^{-1}
LAYERED ICE				
2152	disappears by 80 K	CO-H$_2$O interface	CO-dangling OH[b]	No
2143	requires crystalline CO & polarized light	CO-CO interactions	LO component[c] from LO-TO splitting	Yes
2139	irreversibly shifts & narrows to 2136 (see below) as T raised	CO-CO interactions for layer of CO on H$_2$O	CO-OC-CO[d]	Yes
2139	disappears by 80 K	CO-H$_2$O interface[b]	CO-bonded OH[f]	?[e]
2136	evolves from 2139 band	CO in H$_2$O	?[#]	Yes

[#] Molecular configuration of binding site not yet resolved.

[a] Sandford et al. (1988).

[b] Collings et al. (2003b); Manca et al. (2000); Martin et al. (2002b).

[c] Chang et al. (1988); Collings et al. (2003a).

[d] Ewing & Pimentel (1961); Collings et al. (2003a).

[e] Overwhelmed by pure CO 2139 cm^{-1} band.

[f] This work.

infrared experiments, combined with ab initio calculations assigned the 2139 cm^{-1} band to CO interacting with a dangling OH, but with its O-atom pointing towards the surface (Allouche et al. 1998). In subsequent experiments which included simultaneous volumetric and Fourier Transform infrared isotherm measurements, the 2139 cm^{-1} band was reassigned to CO molecules interacting with the ice surface at low CO coverages and a combination of CO-ice and CO-CO interactions at CO multilayer coverages (Manca et al. 2000, 2001; Martin et al. 2002a,b). The adsorption energy of CO on ice was measured to be about 0.10−0.11 eV (Manca et al. 2001; Martin et al. 2002a,b), in good agreement with earlier measured and calculated values (Allouche et al. 1998; Manca et al. 2000). More recently, temperature programmed desorption and reflection-absorption infrared spectroscopy experiments were performed to study the adsorption and desorption of CO on porous and compact amorphous ices, as well as crystalline ice. In these data the 2139 cm^{-1} band was assigned to CO adsorbed parallel to the ice surface, forming a compact complex with the water molecule (Collings et al. 2003a,b), as discussed in detail in Sect. 4.2. Again, the adsorption energy was measured to be about 0.10 eV (Collings et al. 2003b).

Using results of density functional theory (DFT) quantum calculations on the CO-crystalline ice system, it was suggested that the CO-ice interactions contributing to the 2139 cm^{-1} band are due to CO interacting with the dO and s4 surface adsorbing sites, as shown in Fig. 2 (Manca et al. 2001; Martin et al. 2002b). For the 2152 cm^{-1} band assignment, the DFT calculations corroborated previous evidence that CO is adsorbed perpendicular to the surface, interacting with a dangling OH via its C-atom. From these calculations, the binding energy of the OC-ice configuration was found to be 0.12 eV, compared to 0.07 eV for the CO-ice configuration (Manca et al. 2001). More recently, geometry optimizations were performed employing pair potentials for the CO-H$_2$O interaction to determine the CO adsorbing sites on a static crystalline ice surface, and their corresponding binding energies (Al-Halabi et al. 2003a). The calculations confirm that the most stable configuration corresponds to CO interacting with a dangling OH via its C-atom, associated with the 2152 cm^{-1} band, based on assignments from the experiments mentioned above. CO can also be adsorbed on top of a surface hexagonal ring, interacting with an O-atom of a surface water molecule, whose two hydrogen atoms are involved in the hydrogen bonding network (the dO and s4 sites).

In Sect. 4 of this paper, we relate the previously assigned infrared bands with the binding sites identified from geometry minimizations, to suggest which molecular configurations may be feasibly associated with specific CO-amorphous ice interactions and we discuss how they are related to astronomically observed features.

3. Method

To simulate the adsorption of thermal CO to amorphous ice at T_s = 90 K, classical trajectory calculations were performed (Porter & Raff 1976). Essentially, we followed the same approach as used previously to study the adsorption of HCl

and CO to crystalline and amorphous ice at thermal and hyperthermal energies, where E_i varies between 0.1 and 2.0 eV (Kroes & Clary 1992; Al-Halabi et al. 2001, 2003a,b).

3.1. The ice surface

The amorphous ice surface was modelled using the molecular dynamics method (Allen & Tildesley 1987). The initial configuration was modelled by 6 moving bilayers of crystalline ice. Each bilayer consists of 60 water molecules. The moving bilayers were superimposed on 2 fixed bilayers, containing 120 water molecules, to create an ice slab. The moving water molecules were treated as rigid rotors, but were otherwise allowed to move according to Newton's equations of motion. To simulate an infinite surface at the top of the slab, periodic boundary conditions were applied in directions parallel to the surface (x and y directions). The TIP4P pair potential was used to describe the interactions between the water molecules (Jorgensen et al. 1983).

Starting from a crystalline ice configuration, which obeys the ice rules (Bernal & Fowler 1933) and has zero dipole moment, the amorphous ice slab was equilibrated at T_s = 90 K, in a stepwise fashion. A surface temperature of 300 K was established, using the computational analogue of a thermostat that is applied for about 20 ps (Berendsen et al. 1984). The thermostat was then switched off and the slab was left to equilibrate for about 120 ps. At this temperature (T_s = 300 K), the water molecules behave collectively like a liquid, and they are distributed at random in the slab unit cell (Al-Halabi et al. 2003b). In the second step, the slab temperature was decreased to T_s = 90 K, by imposing the computational thermostat for 15 ps. The slab was then left to equilibrate for another 120 ps before the calculations were performed. This method is similar to that used by Essmann & Geiger (1995) to prepare a "fast quenched" amorphous ice surface.

Two additional methods were also considered here as possible alternative methods for preparing the amorphous ice surface. The first alternative was "slow quenching". In this approach, the slab was warmed to 300 K in sequential steps of 100 K, and then cooled to T_s = 90 K, in steps of 100 and 110 K. At each warming and cooling step, the slab was left to equilibrate for 120 ps. In a third approach, the water molecules were distributed at random in the slab unit cell ("random ice"). Starting from the same "liquid-like" configuration at T_s = 300 K that was used to prepare the "fast quenched" surface, each water molecule was assigned an initial velocity that corresponded to T_s = 10 K, in random directions. The slab was then heated to T_s = 90 K. The "fast quenched" amorphous ice surface was used in the calculations because it most closely resembled the structure of vapor deposited compact amorphous ice obtained experimentally. The "slowly quenched" surface was very ordered and looked similar to a crystalline ice surface. The "random ice" surface was less corrugated than the "fast quenched" surface.

For the amorphous surface, it is rather difficult to define the position of the water molecules at the vacuum-surface interface: the positions of the surface water molecules vary

from about $Z = 23$ Å to 30 Å and the surface is characterized by the presence of several hills and valleys. Here $Z = 0$ Å is defined as the bottom of the two fixed bi-layers, i.e. the base of the ice slab.

The results presented here can be compared with both the astronomical case and laboratory studies on "compact" amorphous ices. The latter are most readily obtained by vapor deposition of H_2O at surface temperatures above 70–80 K. To enable a direct comparison with experiment, a surface temperature of 90 K was used in this study, even though this temperature is higher than the "typical" interstellar case. However, cooling the ice from 90 K to 10 K will not significantly alter the ice morphology and therefore not alter the available binding sites at the surface, nor the results of our simulations. Also, at "warm" temperatures, the adsorbed molecules have sufficient mobility to probe a wider range of adsorption sites of higher binding energies: at $T_s = 10$ K, CO stops at the surface close to where it collides (ballistic deposition) (Collings et al. 2003a,b). The results for CO adsorption to amorphous ice are compared with previous theoretical results obtained for CO interacting with crystalline ice (Al-Halabi et al. 2003b). The Frenkel model (Frenkel 1924) has been used to calculate the CO adsorption lifetime τ at 90 K, and data are then extrapolated to astronomically relevant surface temperatures. Further details are given in Sects. 4.2.2 and 4.3.

3.2. The CO-ice interaction

The interaction between CO and the ice surface has been constructed as a sum of CO-H_2O pair potentials, which are described in detail by Al-Halabi et al. (2003a) and Al-Remawi (2002). In brief, the CO-H_2O pair potential was constructed as the sum of electrostatic, dispersion, and repulsion interactions between CO and H_2O. The CO molecule was modelled by 4 point charges that were obtained by fitting the electrostatic potential of an isolated CO, calculated using the quantum chemistry package GAMESS US (Schmidt et al. 1993) at the MP2 level of theory (Møller & Plesset 1934). The level of theory and the basis sets used ensure that the proper sign of the CO dipole moment is recovered. The dispersion component of the CO-H_2O interaction was obtained from the dispersion part of the Lennard-Jones potential LJ(12-6) between the interacting atoms of the two molecules (Lennard-Jones & Devonshire 1936). The last contribution, due to the short range repulsion interactions between the atoms of CO and those of H_2O, was calculated by fitting ab initio data for four different configurations of the CO-H_2O complex as shown in Fig. 3. The ab initio calculations were performed using the quantum chemistry package GAUSSIAN 98 (Frisch et al. 1998) at the MP2 level of theory (Møller & Plesset 1934). The interaction energies of the CO-H_2O complex were corrected for the basis set superposition error (van Duijneveldt et al. 1994). For the CO-H_2O complex, good agreement between the fitted and the ab initio energies was obtained for the four different configurations studied here, with a maximum underestimate of the binding energy of about 20% in the third configuration shown in Fig. 3c. The interaction between the two molecules is

attractives when CO interacts with the hydrogen atom of the water (Figs. 3c and 3d). For CO interacting with the oxygen atom, the interaction energy is repulsive, as shown in Figs. 3a and 3b. The maximum binding energy of the complex occurs when CO interacts with the H-atom of the water molecule via its carbon atom, as shown in Fig. 3c. In this configuration, CO has a maximum binding energy of 0.06 eV. This value is in good agreement with the available ab initio data (Sadlej & Buch 1994; Allouche et al. 1998). The distance between the center of mass of CO and the oxygen atom of the water molecule is 4 Å and the C–H distance is 2.41 Å, in good agreement with the experimental data (Yaron et al. 1990) and with the results obtained from ab initio calculations (Sadlej & Buch 1994; Allouche et al. 1998).

3.3. The classical trajectory calculations

The H_2O-H_2O and the CO-H_2O interactions in the classical trajectory calculations were set to zero at long intermolecular distances (≥ 10 Å), using a smooth and well-behaved switching function (Kroes & Clary 1992). The initial CO orientation and the impact position on the surface were chosen at random, using the Monte Carlo technique (Allen & Tildesley 1987). In the calculations, 100 trajectories were calculated at normal incidence ($\theta_i = 0°$) for thermal incidence energies (E_i) of 0.01 eV (~ 116 K), with zero initial rotational energy of CO. Each trajectory was run for 15 ps, with a time step of 0.3 fs. At the beginning of each trajectory, CO was placed 11.3 Å above the highest portion of the ice surface and considered to be in the gas phase and infinitely far away from the ice surface. To simulate the collision dynamics, Newton's equations of motion were integrated using an improved leapfrog algorithm (Fincham 1992) for both the impinging molecule and the water molecules.

A trajectory was defined as an adsorbing trajectory if it exhibited more than one turning point in the Z coordinate of CO, for motion normal to the surface, as shown in Figs. 1b and 1c, such that (i) $Z_f \leq 32.5$ Å, where Z_f is the final Z coordinate of CO and (ii) the final energy (E_f) of the adsorbed CO is below kT_s; i.e. $E_f \leq -0.008$ eV. Here E_f of the adsorbed molecule is the sum of its potential, translational and rotational energy. The zero of the CO potential energy is defined by CO being in the gas phase. The alternative to adsorption is that CO scatters directly back from the surface to the gas phase ($Z_f \geq 40.0$ Å), as illustrated in Fig. 1a. On the other hand, the adsorbed molecule may desorb from the physisorbed state back to the gas phase within the lifetime τ, as shown in Fig. 1b, depending on the surface temperature and the binding energy of CO. As will also be shown in Sect. 4.3, τ can often be orders of magnitude longer than the trajectory integration time. Consequently, classical trajectory calculations are often unable to discriminate between trapping desorption (Fig. 1b) and adsorption (Fig. 1c). On the other hand, these mechanisms can often be differentiated from each other on the experimental time scale of a few hours (Gotthold & Sitz 1998; Andersson et al. 2000). In our calculations, the adsorption probability is defined as the ratio of the sum of the adsorbing and trapping desorption trajectories, to the total number of trajectories.

The classical trajectory method is appropriate for studying sticking of molecules like CO to ice surfaces under the conditions considered (E_i = 0.01 eV and T_s = 90 K). Quantum mechanically, sticking is expected to occur predominantly through the excitation of low frequency translational phonons, which have frequencies mostly between 50 and 60 cm^{-1} (between 70 and 90 K) for crystalline ice at T_s = 261 K (Prask et al. 1972). The frequencies should be even lower for the surface phonons. We expect efficient energy transfer to the phonons upon impact and therefore the sticking to be well described by classical mechanics because the effective collision energy (i.e., the collision energy increased by the physisorption energy, which is found to be larger than 450 K, see below) is larger than that corresponding to the frequency of the translational phonons by more than a factor of 7. Quantum reflection from the attractive well is not expected to be a problem at the collision energy and surface temperature considered (see also Slichting et al. 1988).

A potential problem is the neglect of zero-point motion in the classical simulations. In quantum mechanical calculations, adsorption energies are averaged over the surface phonon vibrational wave function, which includes the effect of zero-point vibrations. For the low energy translational phonons, significant averaging is present in the classical simulations because the surface temperature used in the simulations (90 K) exceeds or is equal to the frequency of these phonons. However, there is too little averaging over the higher frequency librations of the water molecules (which peak in the range 100−300 K for crystalline ice (Prask et al. 1972)). As a result, the use of the classical approximation should exaggerate the ability of the adsorbing molecule to localize in a region of coordinate space with low potential, and the calculated adsorption energy is expected to be somewhat too low; i.e. somewhat too negative.

4. Results and discussion

4.1. The ice surface

Top and side views of the simulated amorphous ice slab are shown in Figs. 4a and 4b respectively. The simulated ice slab shows an irregular morphology, with the presence of voids of different sizes. The side view shows that the ice surface is very irregular, with several hills and valleys (Fig. 4b). However, the lower portion of the slab (consisting of the lowest moving water molecules) is more regular, as has also been observed in previous molecular dynamics simulations of amorphous ice (Essmann & Geiger 1995; Masuda et al. 1998). Here, the regularity of the lowest portion of the slab is in part due to the presence of the two fixed bilayers of the water molecules at the base, which have the ordered structure of crystalline ice. The average density of the ice slab is calculated to be about 0.94 g cm^{-3}, in good agreement with the density calculated by Masuda et al. (1998) for low density amorphous (lda) ice (ρ = 0.93 g cm^{-3}) at T_s = 70 K and the value calculated for vapor deposited amorphous ice (ρ = 0.96 g cm^{-3}) (Essmann & Geiger 1995). Experimentally, the density of amorphous solid water (ASW) of different porosities, deposited at T = 22 K, was measured to be between 0.85−1.05 g cm^{-3} (Dohnálek et al. 2003). The computed density of crystalline ice, also
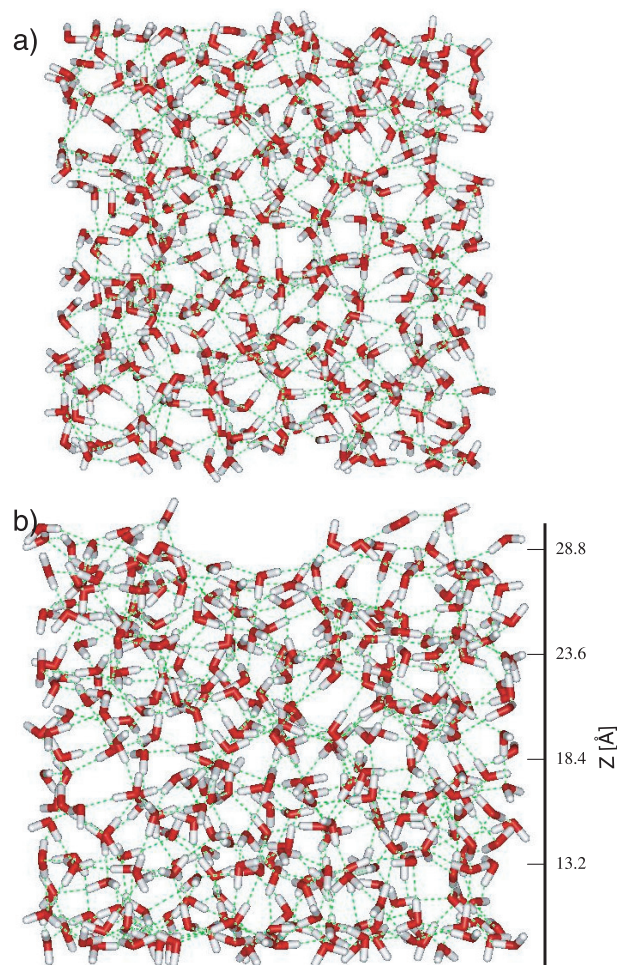

Fig. 4. a) Top (surface) and **b)** side views of the moving water molecules in the amorphous ice slab equilibrated at T_s = 90 K are shown. In the figures, the dark atoms are the oxygen atoms of the water molecules and the light atoms are the hydrogen atoms. The top surface has dimension of 22.48 Å × 23.37 Å (x and y), and the side of the slab has dimension of 22.48 Å × 30.0 Å (x and z). The Z coordinates of the moving water molecules are in the range between 8.2 and 30 Å, where Z = 0 Å is at the bottom of the slab.

equilibrated at T_s = 90 K, was 0.98 g cm^{-3}. This value is higher than the measured density at T_s = 250 K, 0.92 g cm^{-3} (Röttger et al. 1994). However, molecular dynamics calculations using the TIP4P model usually predict higher density values for crystalline ice and water than the measured values (Rick 2001; Jorgensen & Jenson 1998), by about 4−5%.

In our ice structure, each water molecule is labelled as "hb$n$", where n is the hydrogen-bond coordination number (Al-Halabi et al. 2003b). A hydrogen bond is defined to occur between two water molecules if the interaction energy between the two molecules is less than −0.12 eV and lasts for at least 0.5 ps, since a local minimum is found in the pair potential distribution function at this energy. A similar definition of a hydrogen bond has been used previously in a molecular dynamics study on the adsorption of HCl to crystalline ice (Kroes & Clary 1992). In the amorphous ice slab presented here, most of the water molecules are hb4 (about 81%) or hb3 (about 16%) (Al-Halabi et al. 2003b). In the case of a model crystalline ice
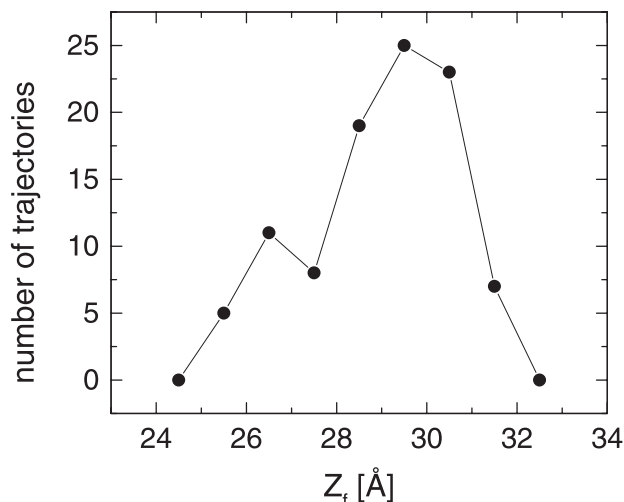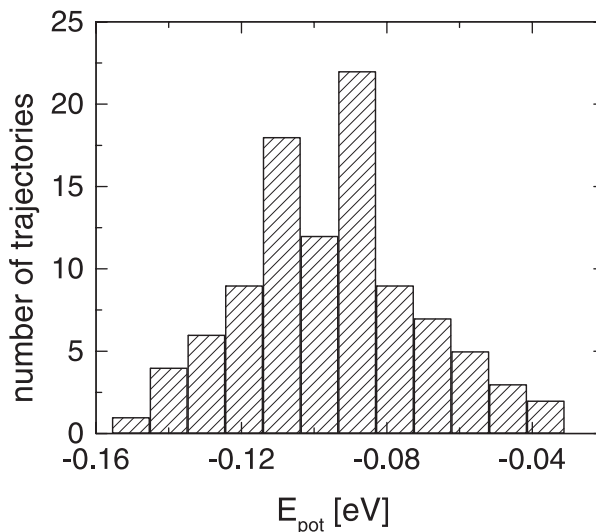
Fig. 5. The number of adsorbing trajectories plotted as a function of Z_f, for CO adsorbed to amorphous ice, at $T_s = 90$ K, with $E_i = 0.01$ eV for normal incidence. The bottom of the ice slab is at $Z = 0$ Å.


Fig. 6. Histograms showing the number of adsorbing trajectories as a function of the final values of E_{pot} of CO, at $T_s = 90$ K, with $E_i = 0.01$ eV, for normal incidence.

slab (without defects), all of the water molecules are hb4, except those in the top monolayer of the surface bilayer, which are hb3. The remaining water molecules in the amorphous ice surface are classified as hb5 (3%), with very small fractions (<1%) of hb2 and hb6. This already suggests that the number of the "dangling OH" sites available for CO adsorption is quite *low*. In fact, the simulations show that, on average, there are *only* about 6 "dangling OH" groups that are accessible to CO at the vacuum-surface interface. For comparison, in the case of a crystalline ice slab, with the same initial *x, y* dimensions, there are, on average, 15 "dangling OH" groups present at the vacuum-surface interface, i.e. half of the hb3 molecules at the surface, as shown in Fig. 3.

4.2. Adsorption

4.2.1. Binding energies

For the thermal incident energies considered here, ($E_i = 0.01$ eV), almost all the trajectories are classified as adsorbing trajectories, with an adsorption probability of 0.99 ± 0.01. Figure 5 shows the number of the adsorbing trajectories plotted as a function of the final height of CO (Z_f), where the bottom of the ice slab is defined to be at $Z = 0$ Å. For all the adsorbing trajectories, a detailed inspection of the trajectories shows that CO is always adsorbed on top of the ice surface, on a surface hill or in a surface valley. Most of the trajectories end with CO being adsorbed at relatively high values of Z_f, on surface hills. At these values of E_i, CO has insufficient energy to penetrate the ice surface or surface valleys with restricted access, i.e., valleys where a barrier needs to be overcome for CO to enter them. In addition, no CO molecules migrated deeper into the surface valleys from their initial impact site, to lower values of Z_f, during the simulation period (15 ps). Temperature programmed desorption experiments performed on CO desorption from compact amorphous ice like that simulated here show that

CO trapping does not occur inside such an ice layer (Collings et al. 2003a). This is in agreement with our dynamical results, where CO diffusion into the slab has not been observed during the simulation.

Elsewhere, it has been shown that even at $E_i = 2.0$ eV and at $T_s = 90$ K, *only* one from 100 trajectories result in CO entering a restricted surface valley, with a barrier to penetration of about 0.4 eV (Al-Halabi et al. 2003a), which is larger than the desorption barrier (~0.1 eV). In the case of crystalline ice, molecular dynamics calculations show that if CO is placed in between the ice bilayers, its potential energy is repulsive by about 0.9–1.0 eV (Al-Halabi et al. 2003b), in agreement with previous ab initio calculations (Allouche et al. 1998). Even at the highest value of E_i considered (2 eV), CO does not penetrate the crystalline ice surface, but rather destroys the surface hexagonal rings (Al-Halabi et al. 2003b). The barrier height for surface penetration to occur varies between 1.85 and 2.90 eV, even when minimized with respect to the CO orientations, which is much higher than the CO desorption energy from the crystalline surface (about 0.1 eV). This implies that CO prefers to be adsorbed on top of the ice surface in pure layers, rather than in an interstitial position inside the H_2O ice slab (as in a mixture), consistent with the observational findings of Pontoppidan et al. (2003).

Figure 6 shows the number of the adsorbing trajectories distributed over the final values of the potential energy of CO (E_{pot}). The average value of E_{pot}, $\langle E_{pot} \rangle$, is −0.094 eV. This is in good agreement with the measured values of about 0.1 eV, obtained from Fourier transform infrared and temperature programmed desorption experiments on CO adsorption to amorphous ice (Allouche et al. 1998; Manca et al. 2000; Martin et al. 2002b; Collings et al. 2003b) and with previous ab initio calculations performed on CO adsorption to hexagonal ice (Allouche et al. 1998; Manca et al. 2001). The figure shows relatively low values of E_{pot} (strong binding to the surface) in
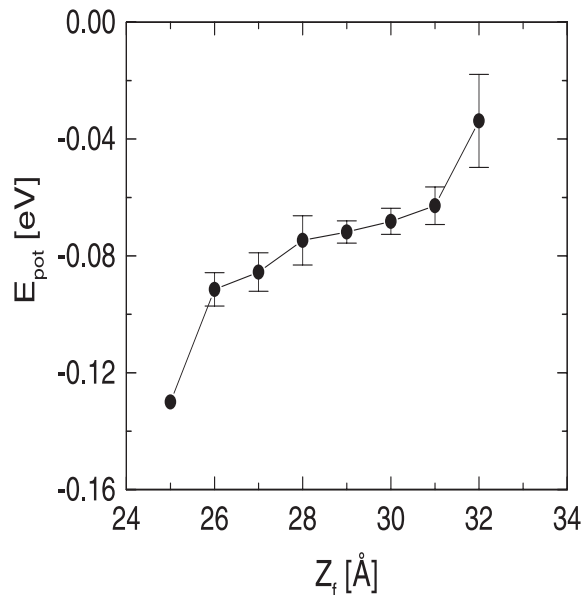
Fig. 7. Final values of E_{pot} of CO plotted as functions of Z_f, for the adsorbing trajectories, at $T_s = 90$ K, with $E_i = 0.01$ eV, for normal incidence.

only few trajectories, with a minimum value of -0.146 eV. As shown below, these lowest values of E_{pot} correspond to the adsorbing sites where CO interacts with the largest number of surface water molecules, for instance when CO is adsorbed in a surface valley, i.e. at low values of Z_f (25–27 Å). There are also a few sites on the amorphous ice surface with high values of E_{pot} (weak binding to the surface), up to -0.04 eV. At these sites, particularly those on top of the surface hills, CO is adsorbed at high values of Z_f and interacts with a smaller number of surface water molecules. This interpretation was confirmed by looking at the dependence of E_{pot} on the final position of the adsorbed CO, Z_f. Figure 7 shows that CO is most strongly bound to the surface at the lowest values of Z_f.

In the case of off-normal incidence, the normal component of E_i, which scales with $\cos^2 \theta_i$, must be transferred to the surface for adsorption to occur. Consequently, at the thermal incidence energies considered here, the dependence of the CO binding energies on incidence angle, θ_i, are expected to be negligible, because the energy to be accommodated at the surface is small compared to the final adsorption energy. For hyperthermal energies (0.5 eV), the dependence of the adsorption probability on θ_i is significant, as has been observed in the case of CO adsorption to crystalline ice (Al-Halabi et al. 2003a). E_{pot} is expected to be independent of θ_i, because the impinging molecule quickly loses the memory of its initial state once it has been adsorbed to the ice surface for a few vibrational periods.

Geometry minimizations of CO interacting with a static, compact amorphous ice surface were carried out to obtain further insight into the possible molecular configurations of the adsorption sites and their corresponding binding energies (E_{pot}). These molecular configurations were obtained by minimizing the interaction energy between CO and the static

ice surface with respect to the CO orientations and positions on top of the ice surface, using the same classical CO-H_2O pair potential that was used in our classical dynamics study (see also Sect. 3.2). The energy minima of CO adsorbed to the static surface were found to lie in the range of -0.155 to -0.066 eV, covering a wider range than that found for CO adsorption to crystalline ice surfaces, where the energy minima of CO lie in the range of -0.147 to -0.096 eV (Al-Halabi et al. 2003b). For amorphous ice, the range of the energy minima is wider because the surface is very irregular, characterized by the presence of several hills and valleys, giving many possible adsorbing sites with different values of E_{pot}. In comparison, the crystalline ice surface is flat, with a long range symmetry that is absent in the case of amorphous ice.

4.2.2. CO adsorbing sites

Figure 8 shows the side views of different CO-ice configurations obtained in geometry minimizations of CO interacting with a static amorphous ice surface, at five different values of $E_{pot} = -0.155, -0.129, -0.111, -0.090,$ and -0.067 eV. In each configuration, CO is shown together with the water molecules present within a sphere of radius 5.0 Å centered at the CO center of mass. The black lines show the interaction between CO and the hydrogen atoms within 3.5 Å, to indicate the coordination number of CO by hydrogen atoms of nearby water molecules. The distance between CO and the closest hydrogen atom is shown in Å. Figure 8a shows the CO-ice configuration with the minimum value of E_{pot}, i.e. the strongest interaction, where CO interacts with a "dangling OH" via its carbon atom, in addition to many "bonded OH" groups. This is consistent with previous experimental and theoretical results (Devlin 1992; Palumbo 1997; Allouche et al. 1998; Manca et al. 2000; Martin et al. 2002a,b; Collings et al. 2003b; Al-Halabi et al. 2003b).

The geometry minimizations show that, on average, E_{pot} decreases as the number of OH groups with which CO interacts increases, i.e. CO is more strongly bound to the surface when it interacts with more OH groups, as shown in Figs. 8a–e. This trend is also in agreement with our dynamical results shown in Fig. 5 and discussed in Sect. 4.2.1. Furthermore, the geometry minimizations show that the adsorption energy difference between CO interacting with primarily a "dangling OH" or with several "bonded OH" groups is often not large, as shown in Figs. 8b and 8c, which have binding energies of -0.129 and -0.111 eV respectively: in Fig. 8b CO interacts with a "dangling OH" group, in addition to two other "bonded OH" groups, whereas in Fig. 8c, CO interacts only with several "bonded OH" groups. Similarly, for crystalline ice, we found that the adsorption energies of CO that correspond to the "dangling OH" and "bonded OH" sites are very similar, with a minimum (most negative) value if CO is adsorbed on a "dangling OH" site (Al-Halabi et al. 2003b).

These results can be compared with those of recent temperature programmed desorption and reflection-absorption infrared spectroscopy experiments on CO adsorption to compact amorphous ice systems (denoted by Collings et al. 2003a as
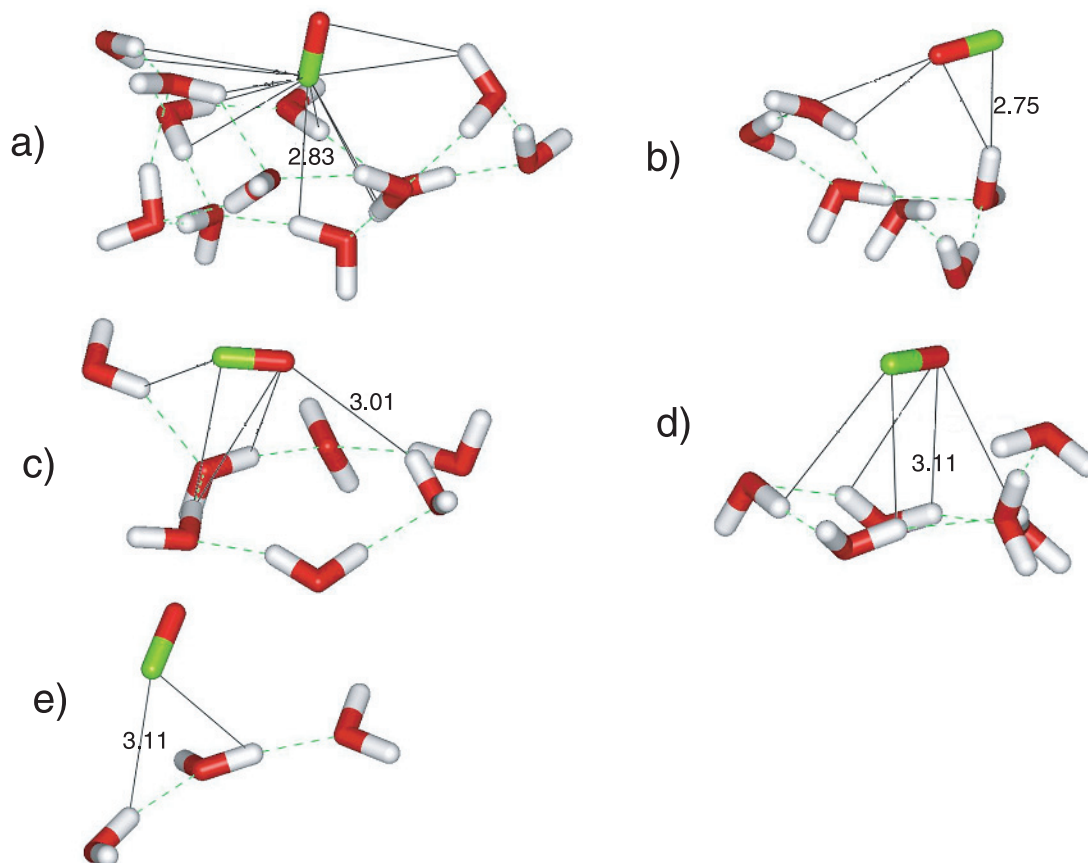
Fig. 8. Examples of CO-static ice configurations, obtained from the geometry optimizations, at five different values of E_{pot}; **a)** −0.155, **b)** −0.129, **c)** −0.111, **d)** −0.090, and **e)** −0.067 eV. Dotted lines show the hydrogen bonding network between the water molecules. Black lines connect CO with the H-atoms (within 3.5 Å), where the shortest distance is given in Å. The color code is the same as in Fig. 3. The 2152 cm^{-1} infrared band is associated with CO interacting primarily with a water molecule with a "dangling OH" as well as those with bonded OH's, as seen in **a)** and **b)**. The 2139 cm^{-1} band is associated with CO interacting with only "bonded OH" water molecules, as shown in **c)**, **d)** and **e)**.

low density amorphous ice I_{lda}). When CO is adsorbed on this ice, the 2152 cm^{-1} band only appears when the temperature is increased from 8 to 25 K, and readily disappears by 50 K. The 2152 cm^{-1} band was assigned by Collings et al. (2003a) to CO adsorbed to a "dangling OH" site, most likely on a hb2 water molecule, which would become more highly coordinated as the ice was warmed, thus accounting for the loss of the binding site. However, our work suggests that only a very few percent of the water molecules in the compact amorphous ice can be classified as hb2, as has been discussed in Sect. 3.1, in agreement with other earlier theoretical studies (Buch 1992; Essmann & Geiger 1995). Consequently it is more likely that the "dangling OH" site will be on a hb3 water molecule, as shown here. In addition, low level ab initio calculations performed with the 3-21G basis set (Collings et al. 2003a) were used to suggest feasible molecular configurations of the CO-H$_2$O surface binding sites observed in these experiments, by looking for the stable CO-H$_2$O gas-phase complex geometries. A linear complex, in which CO interacts with H$_2$O via its oxygen atom (similar to the complex configuration shown in Fig. 3d) and a compact complex, in which the molecular axis of CO is parallel to one of the water OH groups, were found.

The linear complex was suggested to resemble the adsorption site corresponding to the 2152 cm^{-1} band and the compact complex the adsorption site corresponding to the 2139 cm^{-1} band. However, given the low level of these calculations and the fact that only one water molecule is considered, such calculations predicted the complex orientations incorrectly. The geometry minimizations and the molecular dynamics simulations of the amorphous ice surface performed here clearly suggest that the 2152 cm^{-1} band can be associated with CO interacting with a "dangling OH" on hb3 water molecules rather than hb2, and that the 2139 cm^{-1} band can be associated with CO interacting with a "bonded OH", rather like the compact complex described above, although not necessarily with CO parallel to the water OH bond because of the presence of other water molecules.

4.3. Adsorption time

Under interstellar conditions, the build-up of ice layers and subsequent chemical processes at ice surfaces depend on the lifetime (τ) of the adsorbed molecules involved in these processes. Using the classical trajectory method, one can

calculate τ of the adsorbed molecule, by integrating the adsorbing trajectories until the molecule comes back off the surface. An estimate of τ can then be computed by averaging all the adsorption times. However, this is not feasible for most astronomical situations because τ could be orders of magnitude longer than the integration time of the trajectories, as shown in Fig. 1. Instead, we have used the statistical mechanics method established by Frenkel (Frenkel 1924) that is commonly used in astrochemical models (Augason 1970; Goodman 1978; Tielens & Allamandola 1987; Pirronello et al. 1997). Another more accurate method used to calculate τ is the "time" censored maximum-likelihood method (Lawless 1982). This method has been used to estimate τ for CO adsorbed to a crystalline ice surface at $T_s = 150$ K (Gardner et al. 2004). The values of τ obtained with the latter method agree to within a factor of e: $\tau = 390$ ps when Frenkel method is used and 142 ps when the censored maximum-likelihood method is used. On astronomical timescales, such differences are negligible. Assuming that (i) the adsorption probability for CO on amorphous ice is 1.0, (ii) the CO-ice interaction potential depends only on the distance of CO to the surface and (iii) the molecule-surface vibration is harmonic, τ can be estimated, at low CO coverage, from the Frenkel method, by:

$$\tau = \tau_\nu \exp\left(\frac{u}{kT_s}\right) \qquad (1)$$

where τ_ν is the average vibrational period of the adsorbed molecule. For each trajectory, an estimate of the vibrational period was obtained from the adsorption time and the number of turning points in the Z coordinate of CO. Next, τ_ν was computed by averaging these estimates, obtaining $\tau_\nu = 0.95 \pm 0.02$ ps. In Eq. (1), $u = \langle E_{pot}\rangle + \frac{1}{2}kT_s$, where $\langle E_{pot}\rangle$ is taken as a positive number, i.e. the absolute value of $\langle E_{pot}\rangle$, and k is the Boltzmann constant. Applying Eq. (1) at $E_i = 0.01$ eV, $T_s = 90$ K, and with $u = 0.094 + \frac{1}{2}(0.008)$ eV, one obtains $\tau = 287$ ns. Note that the lifetime of CO adsorbed to amorphous ice at $T_s = 90$ K is three orders of magnitude longer than that found for the case of CO adsorbed on crystalline ice at $T_s = 150$ K, where $\tau = 142$ ps (Gardner et al. 2004).

Assuming that $\langle E_{pot}\rangle$ is temperature independent or does not vary significantly with T_s, particularly at low values of T_s, and using the same value for τ_ν obtained here, it is found that τ will be about 10^{28} years if $T_s = 10$ K (much longer than the age of the universe), whereas $\tau = 1$ s if $T_s = 40$ K. These results are in good agreement with the experimental results from temperature programmed desorption and reflection-absorption infrared spectroscopy on the desorption of CO from compact amorphous ice (Collings et al. 2003a). The computed values of τ for $T_s = 40$ K, at the minimum (-0.155 eV) and maximum (-0.066 eV) CO binding energies obtained from the geometry minimizations, are 5.3×10^7 and 4.3×10^{-4} s. The CO molecules become mobile at $T_s > 10$ K and start desorbing at $T_s = 30-50$ K at sub-monolayer coverages (Collings et al. 2003a), in fair agreement with our calculations of the adsorbed CO lifetime. The experiments also show that adsorbed CO molecules on the compact surface are desorbed completely by about $T_s = 50-60$ K.

4.4. Astrophysical implications

The results of the calculations presented here have a number of implications relevant to our understanding of CO-ice interactions in the interstellar medium. First, it has been possible to show that a wider range of binding energies exist between CO and amorphous ice surfaces than between CO and crystalline ice surfaces. Furthermore, when a single CO molecule interacts with a compact amorphous ice surface, the surface-adsorbate interaction involves many water molecules in the surface, rather than just one (see Fig. 8). Here, these interactions have been classified as being dominated by either CO-"dangling OH" or CO-"bonded OH" interactions.

Second, these findings are relevant to our interpretations of observational spectra of solid CO. Together with the previous data on CO-ice systems summarized in Sect. 2.2, these results have been used to reaffirm that the 2152 cm^{-1} infrared band is associated with CO-"dangling OH" interactions, and the 2139 cm^{-1} band with CO-"bonded OH" interactions. At sub-monolayer CO coverages, such interactions would give rise to a stronger infrared feature at around 2139 cm^{-1} than at 2152 cm^{-1}. However, care should be taken when extrapolating these data to the interstellar case, since CO-CO interactions in pure CO ices, and at multilayer CO coverages on H$_2$O ices, *also* give rise to an infrared feature at 2139 cm^{-1} (Collings et al. 2003a) (see Table 1). As discussed previously, recent detections of solid CO towards a large number of young stellar objects have shown that 60% to 90% of solid CO is associated with this "dominant" spectroscopic feature at 2139 cm^{-1} (Pontoppidan et al. 2003). Together with the findings of this work, this suggests that most of the CO must reside in a pure layer of CO, with a small percentage at the CO-ice interface, interacting predominantly with "bonded-OH" groups.

Further evidence for this interpretation comes from the lack of detection of a 2152 cm^{-1} band towards any of the objects observed by Pontoppidan et al. (2003). Our calculations suggest that on compact amorphous ices the number of accessible "dangling-OH" sites is *very low* as discussed in Sects. 4.1 and 4.2.2. Moreover, the difference between the potential energies of the CO-"dangling OH" or CO-"bonded OH" interactions (as shown in Fig. 8) is negligible. Consequently, at $T_s = 90$ K, there is no real energetic advantage in a surface-reconstruction occurring in the compact amorphous ice to make more dangling OH binding sites accessible for CO adsorption at the surface. At $T_s = 10$ K, the H$_2$O molecules may also not possess enough energy for any surface-reconstruction to occur. Given the immobility of CO at $T_s = 10$ K (see Sect. 4.3), it seems very unlikely that a large population of CO molecules will be present at dangling OH binding sites on compact amorphous ice surfaces in the interstellar medium, and indeed, it is then unlikely that one would detect the 2152 cm^{-1} band (Fraser et al. 2003).

However, as discussed below, there is a good chance that interstellar ices are more porous than the compact amorphous ice studied here. As the porosity of the ice increases, so does its total surface area in comparison to the geometric surface area. Therefore, a greater number of water molecules can be considered to be at the surface-vacuum interface, although many

will be in deep valleys or internal surface pores rather than the uppermost external ice surface. Such an ice might therefore be expected to have more dangling OH binding sites per unit geometric surface area than the compact amorphous ice, although the ratio of dangling OH to bonded OH at the surface-vacuum interface itself, is likely to be the same. The question is then whether these sites are accessible to the adsorbing CO. The lack of detection of a 2152 cm^{-1} band suggests they are not, in keeping with the conclusions of a recent discussion of the missing 2152 cm^{-1} band by Fraser et al. (2003).

Conversely, the presence of the 2136 cm^{-1}, associated with CO in H_2O, requires an explanation. Pontoppidan et al. (2003) inferred from their observations of the 2136 cm^{-1} feature that the minimum line-of-sight averaged fraction of CO that could be accommodated in an H_2O matrix is around 16%. In the present dynamical results for $T_s = 90$ K, CO was not observed diffusing into the surface valleys nor penetrating the ice layer after its initial collision with the surface, consistent with the experimental results from compact amorphous ice where no CO trapping was observed (Collings et al. 2003a). However, CO could become mixed within the H_2O matrix if the ice matrix is more porous. Clearly, some CO must become trapped in the pores and valleys as the ice morphology changes, as shown by recent experiments (Collings et al. 2003b). It is not possible from our results to say anything about the binding energies or sites for CO trapped within an H_2O-ice matrix. It is however reasonable to assume that migration into a pore will also not spontaneously occur at $T_s = 10$ K in a porous amorphous ice. Any CO that is later observed trapped in the pores or surface valleys must get there through the collapse of the porous ice, in which grain boundaries become closed off from the surface-vacuum interface. These facts imply that CO always prefers to be adsorbed on top of any ice surface, in pure layers, rather in an interstitial position in a CO-H_2O ice mixture, consistent with observations (Pontoppidan et al. 2003).

One alternative scenario to the trapping scenario presented above is that CO becomes buried within the ice due to simultaneous accretion of CO and H_2O from the interstellar gas. Nothing can be deduced about the binding sites involved from the calculations discussed here, although all the theoretical and experimental evidence suggests that such a configuration is energetically unfavorable. Co-deposition of H_2O and CO in the laboratory always leads to an intense 2152 cm^{-1} band, contradicting observational constraints (Pontoppidan et al. 2003), a strong clue that mixed ices are not a good analogy for the interstellar case. In addition, if H_2O is formed reactively at the grain surface, then CO should be accreted with H and O atoms, not H_2O. One then has to ask why CO depletion in interstellar regions does not correlate with ice growth, occurring across the whole cloud, instead of just in the coldest regions, usually at the cloud-center. Currently, the layered ice and migration model seems to offer the most consistent explanation of interstellar ice behavior, combining theoretical, observational, and experimental evidence.

Finally, the lifetime calculations discussed in Sect. 4.3 reconfirm that at $T_s = 10$ K, the lifetime of the adsorbed CO is long enough for barrierless or low-barrier heterogenous reactions involving CO to proceed on interstellar ice surfaces. For example, the adsorption of CO to ice plays an important role in the formation of CO_2. Most interstellar CO_2 is present in the solid form, with a very low abundance in the gas-phase (van Dishoeck et al. 1996). Like CO, CO_2 is found in hydrogen bonded, H_2O-rich ices and in van der Waals bonded H_2O-poor ices (Gerakines et al. 1999). The most likely pathways for CO_2 formation invoked in astrochemical models involve the heterogeneous CO + OH, CO + O, and HCO + O reactions, which proceed on or in ice surfaces. Given that all these routes depend upon the presence of CO on or in the ice, the adsorption of CO to H_2O ice, and the subsequent lifetime and mobility of the CO molecules on the ice surface must be key to the formation of CO_2. The data presented here and the models and potentials developed for this work can be applied in future theoretical studies of the CO + O and CO + OH reactions at ice surfaces.

5. Conclusions

In this paper, the results of classical trajectory calculations are presented on the adsorption of CO to amorphous ice at $T_s = 90$ K, for thermal normal incidence energy (0.01 eV). The adsorption probability is found to be approximately unity. In all adsorbing trajectories, CO is adsorbed on top of the amorphous ice surface, with $\langle E_{pot} \rangle = -0.094$ eV, in agreement with previous measurements and theoretical calculations. We have not observed any penetration into the ice slab nor into restricted surface valleys, contrary to the case of hyperthermal CO (Al-Halabi et al. 2003b). In addition, CO was not observed to diffuse into the surface valleys on the timescales of our simulations. On average, CO interacts strongly with the ice surface when adsorbed in surface valleys (at low values of Z_f), where it interacts with a large number of water molecules. However, the interaction of CO with the surface becomes weaker when CO is adsorbed on surface hills, where it interacts with a smaller number of water molecules. The geometry minimizations of CO interacting with a static amorphous ice give a wide range of E_{pot} from -0.15 to -0.04 eV, larger than that found for CO interacting with crystalline ice, due to the roughness of the amorphous ice surface.

The maximum values of E_{pot} found in the geometry minimizations of the CO+amorphous ice system occur when CO is adsorbed at a "dangling OH" group, which is associated with the infrared band at 2152 cm^{-1}. In addition, CO interacts with several "bonded OH" groups, associated with the 2139 cm^{-1} band. The new nomenclature introduced here to describe the adsorption sites associated with the infrared bands of solid CO are consistent with the experimental behavior of the two bands based on the type of the surface (porous, compact, or CO-H_2O ice mixture) and on the surface temperature. The computed values of E_{pot} decrease with the number of H_2O molecules coordinating CO, due to stronger interactions with the amorphous ice surface. The small number of "dangling OH" groups at the ice surface potentially explains the absence of this feature in astronomical spectra. The 2139 cm^{-1} band seen in interstellar regions is dominated by the CO-CO interactions but there may be a small contribution from the CO-"bonded OH". Altogether, there is strong

evidence that interstellar CO-H$_2$O ices are predominantly layered rather than mixed. The astronomical 2136 cm^{-1} band is still not understood, and further experimental and theoretical studies are warranted, including molecular dynamics simulations on more porous ice surfaces than those studied here.

The lifetime of CO adsorbed on the surface has been computed at different surface temperatures. At low temperatures, the adsorbed CO is trapped for a very long period of time, enough for the chemical processes to occur if the associated reaction barrier can be overcome. However, the lifetime becomes very short at increasing surface temperatures: at T_s = 40 K, τ = 1 sec and at T_s = 90 K, τ = 300 ns, in agreement with the results of recent temperature programmed desorption experiments (Collings et al. 2003a).

References

Al-Halabi, A., Kleyn, A. W., & Kroes, G. J. 2001, J. Chem. Phys., 115, 482

Al-Halabi, A., van Dishoeck, E. F., Kleyn, A. W., & Kroes, G. J. 2002, J. Phys. Chem. B, 106, 6515

Al-Halabi, A., Kleyn, A. W., van Dishoeck, E. F., van Hemert, M. C., & Kroes, G. J. 2003a, J. Phys. Chem. A, 107, 10615

Al-Halabi, A., van Dishoeck, E. F., & Kroes, G. J. 2003b, J. Chem. Phys., 120, 4263

Al-Remawi, A. 2002, Ph.D. Thesis, Leiden University

Allamandola, L. J., Bernstein, M. P., Sandford, S. A., & Walker, R. L. 1999, Space Sci. Rev., 90, 219

Allen, M. P., & Tildesley, D. J. 1987, Computer Simulations of Liquids (Oxford: Clarendon)

Allouche, A., Verlaque, P., & Pouricin, J. 1998, J. Phys. Chem. B, 102, 89

Andersson, P. U., Någård, & Pettersson, J. B. C. 2000, J. Phys. Chem. B, 104, 1596

Augason, G. C. 1970, ApJ, 162, 463

Berendsen, H. J. C., Postma, J. P. M., van Gunsteren, W. F., DiNola, A., & Haak, J. R. 1984, J. Chem. Phys., 81, 3684

Bernal, J. D., & Fowler, R. H. 1933, J. Chem. Phys., 1, 515

Boogert, A. A., Blake, G. A., & Tielens, A. G. G. M. 2002a, ApJ, 568, 271

Boogert, A. A., Blake, G. A., & Tielens, A. G. G. M. 2002b, ApJ, 577, 271

Boogert, A. A., Tielens, A. G. G. M., Ceccarelli, C., et al. 2000, A&A, 353, 349

Buch, V. 1990, J. Chem. Phys., 93, 2631

Buch, V. 1992, J. Chem. Phys., 96, 3814

Buch, V., Delzeit, L., Blackledge, C., & Devlin, J. P. 1996, J. Phys. Chem., 100, 3732

Buch, V., & Zhang, Q. 1991, ApJ, 379, 647

Chang, H. C., Richardson, H. H., & Ewing, G. E. 1988, J. Chem. Phys., 89, 7561

Chiar, J. E., Adamson, A. J., Kerr, T. H., & Whittet, D. C. B. 1994, ApJ, 426, 240

Chiar, J. E., Adamson, A. J., Kerr, T. H., & Whittet, D. C. B. 1995, ApJ, 455, 234

Collings, M. P., Dever, J. W., Fraser, H. J., & McCoustra, M. R. S. 2003a, Ap&SS, 285, 633

Collings, M. P., Dever, J. W., Fraser, H. J., McCoustra, M. R. S., & Williams, D. A. 2003b, ApJ, 583, 1058

Devlin, J. P. 1992, J. Phys. Chem., 96, 6185

Devlin, J. P., & Buch, V. 1995, J. Phys. Chem., 99, 16534

Dohnálek, Z., Kimmel, G. A., Ayotte, P., Smith, R. S., & Kay, B. D. 2003, J. Chem. Phys., 118, 364

Ehrenfreund, P., Fraser, H. J., Blum, J., et al. 2003, Plan. Space Sci., 51, 473

Ehrenfreund, P., & Schutte, W. A. 2000, in Astrochemistry: From Molecular Clouds to Planetary Systems, 197, 135

Essmann, U., & Geiger, A. 1995, J. Chem. Phys., 103, 4678

Ewing, G. E., & Pimentel, G. C. 1961, J. Chem. Phys., 35, 925

Fincham, D. 1992, Mol. Simul., 8, 165

Fraser, H. J., Collings, M. P., Dever, J. W., & McCoustra, M. R. S. 2003, MNRAS, submitted

Frenkel, J. 1924, Z. Phys., 26, 117

Frisch, M. J., Trucks, G. W., Schlegel, H. B., et al. 1998, Gaussian, Revision A.5 (Pittsburgh PA: Gaussian, Inc.)

Gardner, D. O. N., Al-Halabi, A., & Kroes, G. J. 2004, J. Phys. Chem. B, 108, 3540

Gerakines, P. A., Whittet, D. C. B., Ehrenfreund, P., et al. 1999, ApJ, 522, 357

Goodman, F. O. 1978, ApJ, 226, 87

Gotthold, M. P., & Sitz, G. O. 1998, J. Phys. Chem. B, 102, 9557

Graham, A. P., Menzel, A., & Toennies, J. P. 1999, J. Chem. Phys., 111, 1169

Hagen, W., Tielens, A. G. G. M., & Greenberg, J. M. 1981, Chem. Phys., 56, 267

Hixson, H. G., Wojcik, M. J., Devlin, M. S., Devlin, J. P., & Buch, V. 1992, J. Chem. Phys., 97, 753

Jorgensen, W. L., Chandrasekhar, J., Madura, J. D., Impey, R. W., & Klein, M. L. 1983, J. Chem. Phys., 79, 926

Jorgensen, W. L., & Jenson, C. 1998, J. Comp. Chem., 19, 1179

Kimmel, G. A., Dohnálek, Z., Stevenson, K. P., Smith, R. S., & Kay, B. D. 2001, J. Chem. Phys., 114, 5259

Kroes, G. J., & Clary, D. C. 1992, J. Phys. Chem., 96, 7079

Lawless, J. F. 1982, Statistical Models and Methods for Lifetime Data (New York: Wiley)

Lennard-Jones, J. E. & Devonshire, A. F. 1936, Nature, 137, 1069

Manca, C., & Allouche, A. 2001, J. Chem. Phys., 114, 4226

Manca, C., Martin, C., Allouche, A., & Roubin, P. 2001, J. Phys. Chem. B, 105, 12861

Manca, C., Roubin, P., & Martin, C. 2000, Chem. Phys. Lett., 330, 21

Martin, C., Manca, C., & Roubin, P. 2002a, Surf. Sci., 502-503, 275

Martin, C., Manca, C., & Roubin, R. 2002b, Surf. Sci., 502-503, 280

Masuda, K., Takahashi, J., & Mukai, T. 1998, A&A, 330, 773

Møller, C., & Plesset, M. S. 1934, Phys. Rev., 46, 618

Palumbo, M. E. 1997, J. Phys. Chem. A, 101, 4298

Petrenko, V. F., & Whitworth, R. W. 1999, Physics of ice (Oxford: University Press)

Pirronello, V., Biham, O., Liu, C., Shen, L., & Vidali, G. 1997, ApJ, 483, L131

Pontoppidan, K. M., Fraser, H. J., Dartois, E., et al. 2003, A&A, 408, 981

Porter, R. N., & Raff, L. M. 1976, Dynamics of Molecular Collisions, Part B, ed. W. H. Miller (New York: Plenum)

Prask, H. J., Trevino, S. F., Logan, K. W., & Gault, J. D. 1972, J. Chem. Phys., 56, 3217

Rick, S. W. 2001, J. Chem. Phys., 114, 2276

Röttger, K., Endriss, A., Ihringer, J., Doyle, S., & Kuhs, W. F. 1994, Acta Crystallogr. B, 50, 644

Sadlej, J., & Buch, V. 1994, J. Chem. Phys., 100, 4272

Sandford, S. A., Allamandola, L. J., Tielens, A. G. G. M., & Valero, G. J. 1988, ApJ, 329, 498

Schmidt, M. W., Baldridge, K. K., Boatz, J. A., et al. 1993, J. Comput. Chem., 14, 1347

Slichting, H., Menzel, D., Brunner, T., Brenig, W., & Tully, J. C. 1988, Phys. Rev. Lett., 60, 2515

Takahashi, J., Masuda, K., & Nagaoka, M. 1999a, ApJ, 520, 724

Takahashi, J., Nagaoka, M., & Masuda, K. 1999b, MNRAS, 306, 22

Takahashi, J., & Williams, D. A. 2000, MNRAS, 314, 273

Tanaka, M., Nagata, T., Sato, S., & Yamamoto, T. 1994, ApJ, 430, 779

Tielens, A. G. G. M., & Allamandola, L. J. 1987, in NATO ASIC Proc. 210: Physical Processes in Interstellar Clouds, 333

Tielens, A. G. G. M., Tokunaga, A. T., Geballe, T. R., & Baas, F. 1991, ApJ, 381, 181

van Dishoeck, E. F., Helmich, F. P., de Graauw, T., et al. 1996, A&A, 315, L349

van Duijneveldt, F. B., van Duijnevelt-van De Rijdt, J. G. C. M., & van Lenthe, J. H. 1994, Chem. Rev., 94, 1873

Whittet, D. C. B., Gerakines, P. A., Tielens, A. G. G. M., et al. 1998, ApJ, 498, L159

Yaron, D., Zolandz, D., Peterson, K. I., et al. 1990, J. Chem. Phys., 92, 7095

Zhang, Q., & Buch, V. 1990, J. Chem. Phys., 92, 5004